*Earth Surface Processes and Landforms*
*Earth Surf. Process. Landforms* **28**, 87–98 (2003)
Published online in Wiley InterScience (www.interscience.wiley.com). DOI: 10.1002/esp.432

# RECENT VENTIFACT DEVELOPMENT ON THE CENTRAL OREGON COAST, WESTERN USA

JASPER KNIGHT[1]* AND HELENE BURNINGHAM[2]

[1] *Glacial Research Group, School of Biological and Environmental Sciences, University of Ulster, Coleraine, Co. Londonderry, BT52 1SA, UK*
[2] *Coastal & Estuarine Research Unit, Department of Geography, University College London, Chandler House, 2 Wakefield Street, London WC1N 1PG, UK*

*Received 29 October 2001; Revised 13 June 2002; Accepted 25 July 2002*

## ABSTRACT

The unusual location of ventifacts, on a boulder-built jetty at the mouth of the Siuslaw River, Oregon coast, western USA, allows ventifact age and wind abrasion rates to be estimated with some precision. The jetty was built mainly between 1892–1901 and extended throughout the twentieth century. Consideration of historical shoreline position and the history of jetty construction and repair suggests the ventifacts have formed since about 1930.

Morphologically the ventifacts are aligned south-to-north reflecting winter winds and sediment transport from the adjacent beach. Wind-parallel grooves and ridges with sharp, sinuous crests are developed on inclined boulder surfaces on top of the jetty and reflect suspended sand transport in wind vortices. Deeply pitted surfaces on steep boulder surfaces nearest the beach reflect impact by saltating sand grains.

Based on present wind regimes (1992–2000) from three regional weather stations, southerly winds above the sand transport threshold occur for 21·9–29·6 per cent of the time. Based on estimated depth of loss from boulder surfaces, wind abrasion rates are calculated to be on the order of 0·24–1·63 mm $a^{-1}$. This is the first well-constrained field estimate of ventifact age and ventifaction rate from a modern coastal environment. 

KEY WORDS: ventifacts; Oregon; wind transport; wind abrasion rates; coastal dynamics

## INTRODUCTION

Ventifacts (wind-etched clasts or bedrock surfaces) are features found commonly in modern coastal environments where loose intertidal and supratidal sand can be blown onto and abrade adjacent rocks and boulders (King, 1936; Greeley and Iversen, 1985; Bishop and Mildenhall, 1994; Braley and Wilson, 1997). Despite many field observations of ventifacts from coastal and inland (arid and semi-arid) environments, however, there have been few estimates of the time-scale required for ventifaction (the process of ventifact development). Reasons for this may include the poorly defined and qualitative visual basis on which ventifacts are identified (Miotke, 1982), the range of possible time-scales (hours to millennia) on which ventifaction can take place (Kuenen, 1960; Miotke, 1982), and the relict nature of some ventifacts with respect to present-day winds (Schlyter, 1995). Ventifaction is also dependent on a range of environmental variables including wind approach angle and its constancy over time, sediment grain size and concentration in the windstream, and rock surface hardness (Schoewe, 1932; Lancaster, 1984; Greeley and Iversen, 1985), characteristics which are difficult to evaluate in the field. Accurately ageing ventifacts in the field is also necessary in order to quantify wind abrasion rates. An experimental plot set up by Sharp (1964, 1980) in an inland, semi-arid environment yielded abrasion rates which varied by a factor of four over different time-periods and on different lithologies.

This present study uses historical, map and field data to evaluate ventifact development in a modern coastal environment in central Oregon, western USA. The unique setting of the ventifacts, on a boulder-built jetty which has a known construction and repair history, allows a detailed estimate of the time-period required for ventifact development, and thus estimates of modern wind abrasion rates.

* Correspondence to: Jasper Knight, School of Biological and Environmental Sciences, University of Ulster, Coleraine, County Londonderry, Northern Ireland, BT52 1SA, UK. E-mail: j.knight@ulst.ac.uk

## COASTAL GEOMORPHOLOGY AND PRESENT-DAY COASTAL DYNAMICS

The tectonically active Oregon coast is mesotidal, north–south aligned, and comprises isolated bedrock headlands separated by long, dissipative beaches which are often associated with river mouths and estuaries (Figure 1). Sand dunes and sandy beaches, present along 45 per cent of the Oregon coast (Cooper, 1958), were formed when sediments were worked onshore during Holocene sea-level rise (Clemens and Komar, 1988; Komar, 1997). The coast between Coos Bay and Florence (85 km long) contains 85 per cent of Oregon's active coastal dunes (USDA, 1975) (Figure 1). This region (Oregon Dunes National Recreation Area, ODNRA) exhibits shore-parallel and generally continuous foredunes (<50 m high) which are backed by wet deflation plains and interdune slacks, hummocky erosional dune remnants and blow-outs, exposed unstable sand, and newly stabilized dunes. The foredunes are generally vegetated by European marram grass (*Ammophila arenaria*) and developing scrub woodland, and fronted by small (a few metres in height), mobile and partially vegetated sand hummocks. The supratidal zone is dominated by sand 'sheets' and mobile, unvegetated asymmetric barchanoid and linguoid dunes (<1·5 m high, 6 m long). These bedforms are linked dynamically to seasonal changes in wind strength and direction (Fox and Davis, 1978; Hunter *et al*., 1983). The northernmost part of the ODNRA dune system, adjacent to the mouth of the Siuslaw River (Figures 1, 2), is characterized by low elevation (<1·5 m high) dune mounds separated by unvegetated slacks which are infilled with sand sheets.

Present-day sediment dynamics of the Oregon coast are controlled mainly by seasonal changes in wind and wave climates (Fox and Davis, 1978; Hunter *et al*., 1983). The present-day beach is in sediment equilibrium (Komar, 1997) and the shore-parallel morphology and continuity of foredunes suggests mainly onshore–offshore sediment transport vectors. Despite the strong evidence for supratidal sand transport by winds (presence of dunes and migratory bedforms fronting the foredunes), it is likely that sand input by tidal pumping offshore from the Siuslaw River is redistributed away from the jetties and deposited onshore by tidal currents (Komar *et al*., 1976).

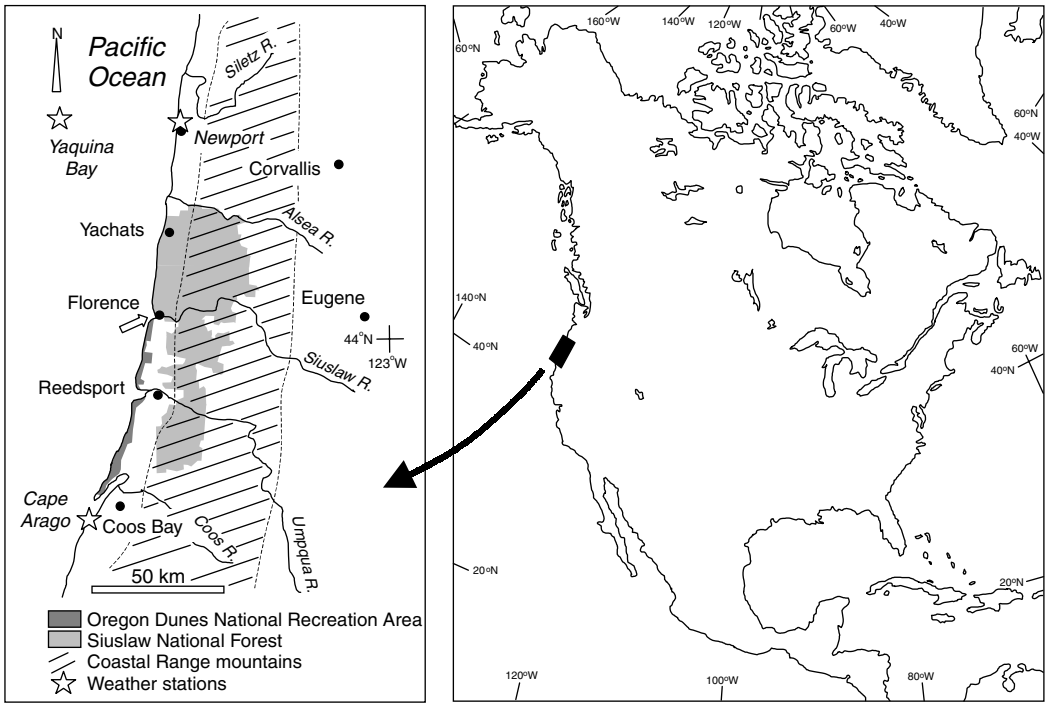


Figure 1. Location of the Siuslaw River near Florence at the northernmost end of the Oregon Dunes National Recreation Area (arrowed) along the central Oregon coast, western USA, and the location of weather stations used in this study

 

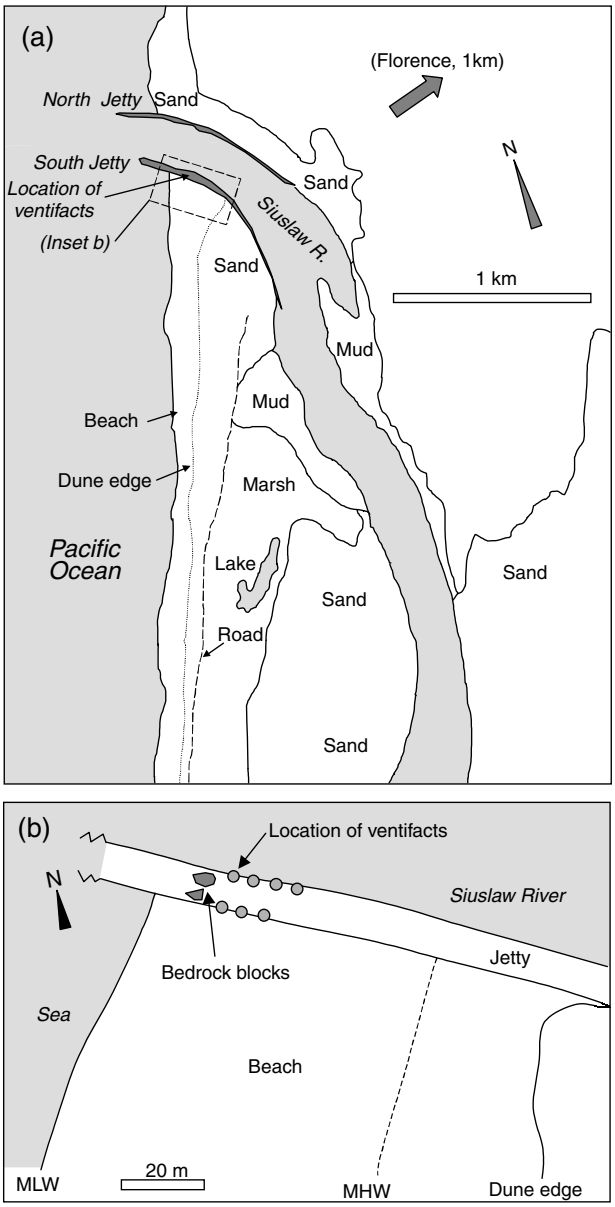


Figure 2. (a) Coastal morphology near the mouth of the Siuslaw River as mapped from aerial photos (29 March 1974, scale 1 : 31 680) (USDA, 1975). (b) Sketch of the location of ventifacts with relation to the jetty and the beach intertidal zone

*Wind climate patterns: methods and results*

The present wind climate of this region, and synoptic wind flow patterns of the western North American coast as a whole, has a pronounced seasonal pattern (Bond *et al*., 1996; Mass and Bond, 1996) (Figures 3, 4). No long-term wind data are available from the study area itself. Rather than use long-term wind records from a single site elsewhere, which may be unrepresentative of winds in the study area, we examined wind records from three regional weather stations, all of which are approximately equidistant from the study area (Figure 1, Table I). Areas of agreement or disagreement between these three records may suggest confidence or caution in the use of records from single sites. The wind data examined are for the time period 1 January 1992 to 31 December 2000 inclusive and were taken from the National Data Buoy Center (downloadable

 

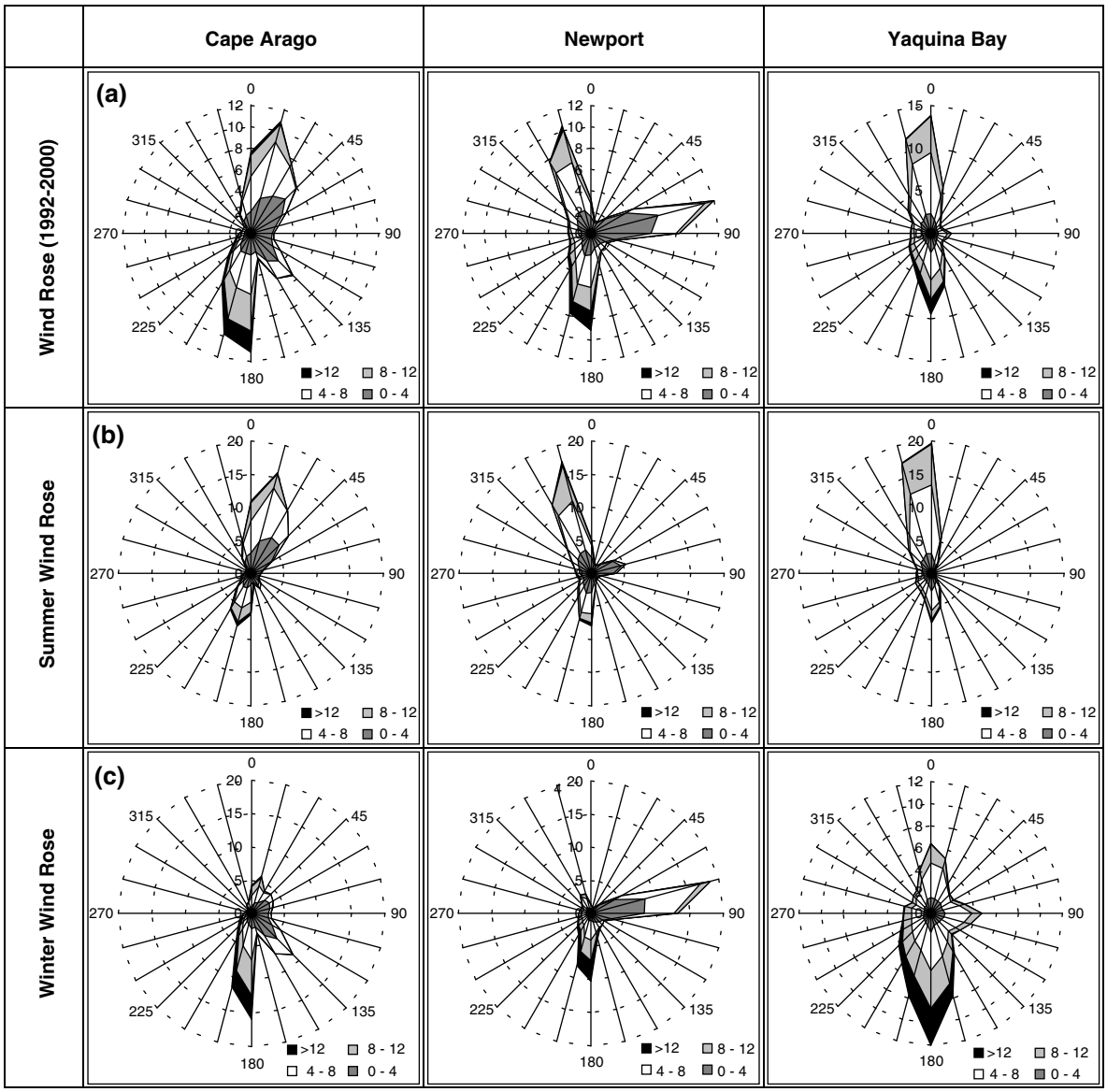


Figure 3. Rose diagrams of wind data for Cape Arago, Newport and Yaquina Bay for the period 1992–2000 inclusive. (a) Frequency of total annual wind speeds in the datasets (m $s^{-1}$) grouped into speed bands of 4 m $s^{-1}$ and plotted by wind direction ($^{o}$N) for the three stations; (b) summer (April–September inclusive) wind speeds (m $s^{-1}$) plotted by wind direction ($^{o}$N) for the three stations; (c) winter (October–March inclusive) wind speeds (m $s^{-1}$) plotted by wind direction ($^{o}$N) for the three stations

at http://www.ndbc.noaa.gov/Maps/rmd.shtml). The raw data, comprising hourly wind directions (in single degrees) and wind speeds (in m $s^{-1}$), were grouped into summer (April–September inclusive) and winter periods (October–March inclusive) (Table II, Figure 3). Using a MATLAB program, the wind direction data were further grouped into 15° classes and wind speed data (resolution of 0·1 m $s^{-1}$) grouped into classes with increments of 4 m $s^{-1}$, deriving the wind roses displayed in Figure 3. Assessment of the frequency of wind directions and speeds is based on analysis of the raw data.

At all stations, winds are dominantly meridional with winds from the northerly quandrant during the summer (44–57 per cent of all summer winds) and winds from the southerly quadrant during the winter

 


Figure 4. (A) Photo of the south jetty, Siuslaw River, from the southeast, showing the broad, sandy beach and hummocky proto-dunes (foreground) vegetated by *A. arenaria*. The large boulders in photo B are arrowed here. People on the beach (circled) for scale. (B) Photo of the supratidal area of the beach and south jetty from the southeast (large boulders arrowed as in photo A) showing mobile sand sheets and streaks, the location of mean high water (MHW; dotted line), the extent of ventifacts along the jetty (double arrow) and the location of surface sand sample (filled circles). Surfer on beach for scale

Table I. Weather station location and characteristics (from National Data Buoy Center, accessible through http://www.ndbc.noaa.gov/Maps/rmd.shtml)

| Station characteristics | Cape Arago | Newport | Yaquina Bay |
|---|---|---|---|
| Station code | CARO3 | NWPO3 | Buoy 46050 |
| Distance from study area | 75 km SSW of Florence | 69 km N of Florence | 79 km NW of Florence |
| Location | 43°20′24″N, 124°22′48″W | 44°36′36″N, 124°4′12″W | 44°37′12″N, 124°31′48″W |
| Site elevation | 18.0 m above sea level | 9.1 m above sea level | Sea level |
| Anemometer height | 14.9 m above site elevation | 9.4 m above site elevation | 5 m above site elevation |

(33–53 per cent of all winter winds) (Table II). Easterly winds during the winter are present at Newport (less so at Cape Arago) but are less pronounced from the offshore Yaquina Bay record (Figure 3). These easterlies are interpreted as orographic-driven offshore winds exiting through valleys of the Coastal Range mountains (Mass and Bond, 1996). Wind speeds are similar between the onshore stations but are higher offshore. The marked seasonal pattern of wind directions, which is consistent between the records despite their geographical spread (50–150 km apart), suggests these records can be used with confidence to provide gross (seasonal and regional-scale) wind climate conditions in the study area.

 

Table II. Analysis of wind data from the chosen weather stations (Figure 1). Wind speeds in the raw datasets are to the nearest 0·1m $s^{-1}$ and so percentages were calculated from a $V_t$ of 2·8 m $s^{-1}$

| | Cape Arago | Newport | Yaquina Bay |
|---|---|---|---|
| Summer | | | |
| Mean wind speed (m $s^{-1}$) | 4·3 | 4·4 | 5·3 |
| % of northerly winds (NW–NE) | 54·1 | 44·8 | 57·6 |
| % of southerly winds (SW–SE) | 30·1 | 27·2 | 26·7 |
| % of wind speeds >2·8 m $s^{-1}$ | 63·5 | 61·1 | 78·3 |
| Winter | | | |
| Mean wind speed (m $s^{-1}$) | 5·1 | 5·5 | 6·7 |
| % of northerly winds (NW–NE) | 22·1 | 13·7 | 26·0 |
| % of southerly winds (SW–SE) | 53·7 | 33·9 | 43·7 |
| % of wind speeds >2·8 m $s^{-1}$ | 71·7 | 72·8 | 85·2 |
| All | | | |
| % of time wind speeds >2·8 m $s^{-1}$ | 67·5 | 66·8 | 81·4 |
| % of time wind speeds >2·8 m $s^{-1}$ from north (NW–NE) | 25·2 | 19·8 | 35·7 |
| % of time wind speeds >2·8 m $s^{-1}$ from south (SW–SE) | 29·6 | 21·9 | 26·2 |

## VENTIFACT SETTING

Ventifacts are located on the south jetty of the Siuslaw River, south of the city of Florence (Figure 2), which marks the northernmost limit of the ODNRA. The jetties on the northern (total 2970 m long) and southern (total 1900 m long) sides of the river were constructed by the US Army Corps of Engineers (USACE) in the period 1892–1901 and 1910–1913 respectively, and both were extended to 65–80 per cent of their present length in the period 1912–1917. Since that time both jetties have been repaired at about 30-year intervals, most recently in the period 1984–1985 when they were extended to their present lengths. The earlier jetties were built mainly from sandstone boulders; more recent repairs and extensions to the south jetty are of diabase. Both lithologies are present on the jetty surface. The jetties have a rhomboid shape in section and are 35 m wide and 6 m high at mean low water. The south jetty is composed mainly of quarried bedrock boulders (0·5–2·5 m diameter) of both sandstone and diabase. The boulders are equant, angular to subangular and generally arranged such that the biggest boulders form the base of the jetty with smaller ones on top giving a relative relief of up to 0·5 m. Boulders of both lithologies are massive and show few or no lines of weakness such as joints. The jetty is morphologically uniform along its length and the top of the jetty (10 m wide) is slightly cambered and infilled with rubble for vehicle access. Morphological stability of the south jetty surface and its constituent boulders is demonstrated by the presence of a USACE survey marker (dated 1970) embedded within the upper surface of a boulder near the top of the jetty.

The south jetty extends offshore from near the stabilized foredunes (Figure 2b). The width of beach exposed adjacent to the jetty varies between *c*. 30–100 m according to tide state, and jetty boulders protrude 1–3 m above beach level, generally increasing in height in a seaward direction (Figure 4). Surface sand samples taken from the beach are unimodal, medium-grained and well-sorted (mean 216 μm). No samples ($n = 3$; locations in Figure 4B) contained particles <90 μm or >500 μm.

## DESCRIPTION OF VENTIFACT MORPHOLOGY

Ventifacts are located along a 30 m long section of the south jetty on the beach-side and top of the jetty (Figures 2, 4), and are developed to an equal extent on both sandstone and diabase boulders, although the sandstone boulders are relatively infrequent (*c*. 20 per cent). All ventifacted surfaces observed were on south-facing boulder surfaces. Three main ventifact styles are recorded (grooves and ridges, pits, polish; *sensu* Greeley and Iversen, 1985) which relate broadly to the position of the boulders with relation to sand source

 

and the local wind stream. Some boulders show both polishing and pitting; no boulder shows both grooving and pitting.

Boulders with grooved and ridged faces are found mainly (12 of 14 occurrences), and are best developed, on the top of the jetty and near its northern flank adjacent to the Siuslaw River. Grooves and ridges are present on the sloping, south-facing flanks of these boulders (Figure 5A). The ridges are sharp-crested, straight to slightly sinuous with a vertical relief of <2·5 cm, and are spaced 6–30 cm apart. The ridge crests are aligned towards 000–015° and generally increase in prominence up the boulder face. Figure 5A shows development from undulating grooves with a spacing of *c*. 1 cm and <5 mm relief (below the trowel in Figure 5A) to the sharp-crested ridges which have a wind-parallel alignment. On this boulder, these ridges terminate at a sharp west–east aligned keel which is left overhanging as a result of undercutting (on the far top left of the boulder; Figure 5A). Other boulders show small feather-like grooves (spacing of <5 mm; a few millimetres of microrelief) which also increase in relief and fan out up the boulder face.

Boulders with pitted faces are found mainly (nine of ten occurrences) on the southern flank of the jetty adjacent to the beach (Figure 5B–D). Pits are best developed on the south-facing sides of individual boulders at or above the present sand surface. Boulder tops show no pitting or ventifaction of any sort. The pits have a range of morphological forms which change according to the orientation of the boulder surface. Some small pits (depth and diameter of a few millimetres) are developed uniformly across boulder faces where pits are aligned perpendicular to the orientation of the wind-facing boulder surface (Figure 5B). Pits developed at an angle to the boulder surface form a rill-like pattern and are thus transitional to grooves (Figure 5C). These pits generally have a jagged up-stream side and smooth down-stream side and may pick out irregularities in boulder surface texture or mineralogy. The pits and rills are a few millimetres in depth and <1 cm long. Other pits do not show a strong orientation and form undulating rills or asymmetric, downward-pointing, lobe-shaped pits across the boulder surface (Figure 5D). Pits of all morphologies are developed exclusively on south-facing boulder flanks; no pits are observed elsewhere on the boulders. The contrast between ventifacted and non-ventifacted boulder surfaces can be clearly seen in Figures 5C and 5D. Less commonly (15 per cent of all ventifacted boulders), polished surfaces are present. Polishing occurs across all exposed surfaces on some mainly fine-grained boulders which are edge-rounded and have a low surface relief.

## DISCUSSION

### *Formation of ventifacts*

Together, the morphology and alignment of ventifacts on the Siuslaw River jetty record a consistent south-to-north wind transport of sand from the adjacent beach. Ventifact morphology strongly reflects the angle of wind impact on the boulder surface. Wind-parallel grooves and ridges are present on inclined boulder faces (<30°). Grooves and ridges develop by sand transport within stable helicoidal vortices across moderately inclined surfaces (Maxson, 1940; Laity, 1987). Wind vortices may be funnelled by boulder microtopography (Whitney and Dietrich, 1973; Ritter and Dutcher, 1990). The undercut ventifact keel (Figure 5A) may represent the unstable break-up of these vortices, especially since the ridges and grooves converge up the boulder face (Figure 5A). The steeply dipping, pitted boulder faces record impact by sand grains in saltation and suspension transport (Sharp, 1949, 1964). The asymmetric lobe-shaped pits may indicate sand impact by saltation rather than through suspended sediment transport. This interpretation is consistent with ventifacts observed in sand-abundant semi-arid and arid settings (e.g. Sharp, 1964, 1980; Lancaster, 1984).

A schematic model illustrating ventifact formation at the site is shown in Figure 6. Here, southerly winds impact the southern side of the jetty at a high angle, giving rise to pitted boulder surfaces. Sand transport is mainly through saltation or as a dense traction carpet, forming the mobile supra- and intertidal dunes and onlapping sand sheets (seen in Figure 4B). Across the top of the jetty, sand transport is mainly by suspension or modified saltation by sand grains in low density in the windflow. Free windflow across boulder upper surfaces is indicated by the formation of grooves and ridges (Figure 5A) which may indicate the presence of helicoidal vortices (Fisher, 1996). This strong relationship between wind approach angle with respect to the boulder face, and resultant ventifact style, has been noted by several authors (e.g. Kuenen, 1928; Blackwelder, 1929; Greeley and Iversen, 1985). However, there is a notable continuum of forms between pit and groove

 

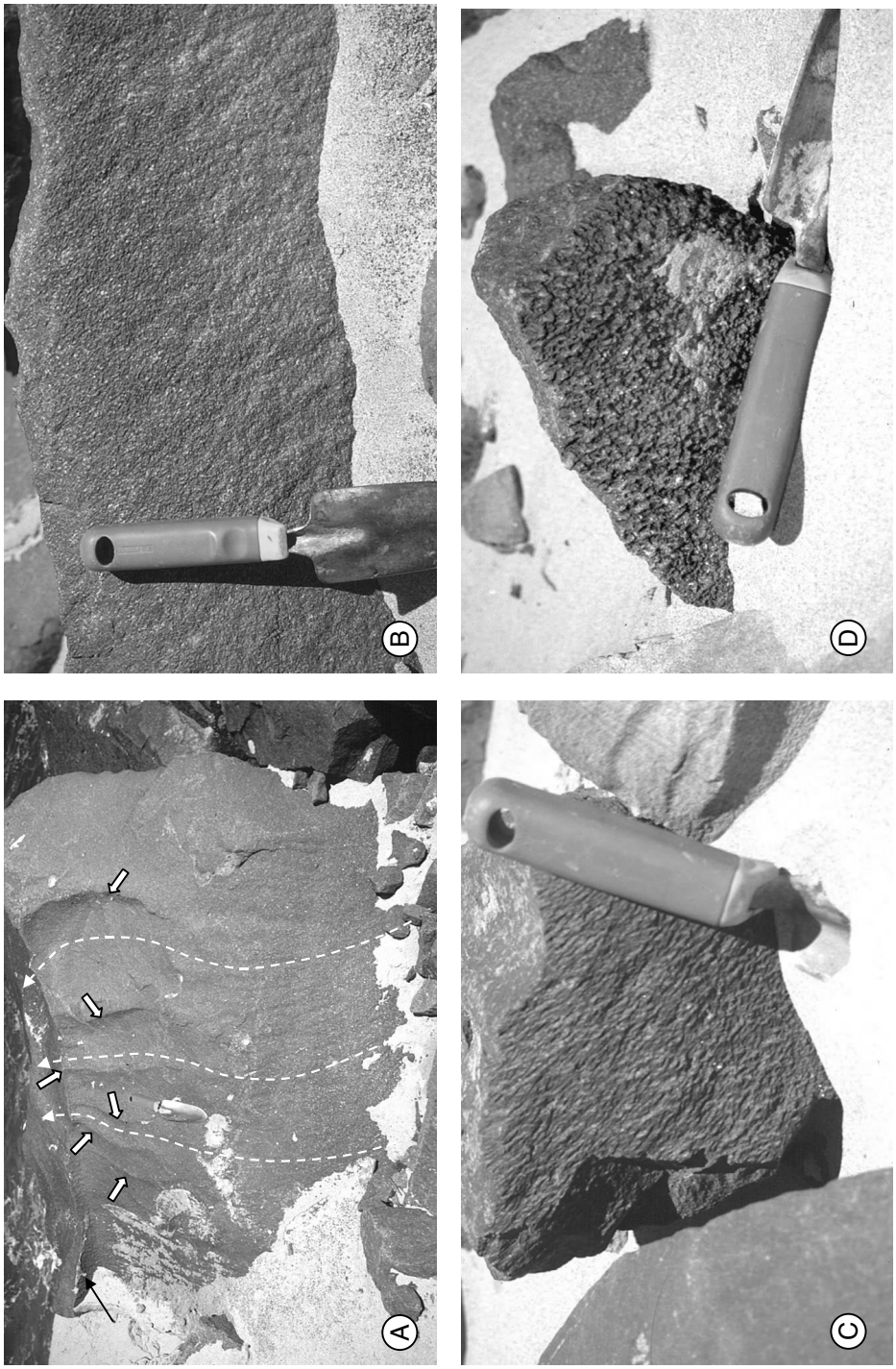


Figure 5. Detailed photos of ventifacts on the south jetty. Trowel for scale is 28 cm long. (A) Wind-parallel ridges (up to 3 cm deep, 10–40 cm apart) and grooves developed on a sandstone boulder. Ridge crests (marked with white arrows) develop in relief up the boulder face. Dotted arrows show the direction of prevailing wind. The sharp boulder keel is undercut to the left (black solid arrow). (B) Small pits (few millimetres in dimensions and depth) developed at ground level on a diabase boulder. (C) Elongate, rill-like pits (up to 8 mm long, 5 mm deep) developed at ground level on a diabase boulder. (D) Downward-pointing lobe-like asymmetric pits (up to 6 mm across, 4 mm deep) developed on a diabase boulder. Note the contrast of wind abrasion between the boulder's upper and flanking surfaces

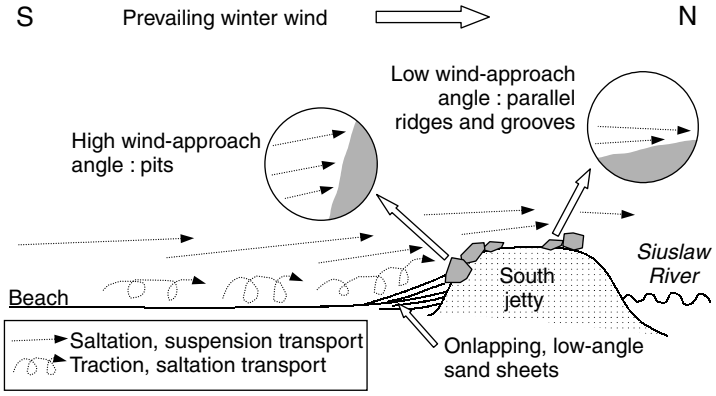


Figure 6. Model for the development of different ventifact shapes at different positions on the south jetty with respect to prevailing wind direction. No spatial scale is implied

end-members (e.g. Figure 5C). Here, asymmetric forms develop where wind abrasion picks out irregularities in rock texture (e.g. Blackwelder, 1929; Suzuki and Takahashi, 1981; Lancaster, 1984) but where the dominant abrasion process is saltation rather than suspension transport. Symmetric forms develop from suspended sand transport across moderately inclined faces.

*Modern changes in coastal morphology and likely age of ventifacts*

Komar *et al.* (1976) presented mapped shoreline positions around the Siuslaw River mouth between 1889 and 1974 (i.e. before and after building and progressive extension of the north and south jetties). Until 1939 these maps show general seaward beach accretion (up to a total of 600 m) on either side of the jetties, mirroring the periods of jetty extension (Komar *et al.*, 1976; Komar, 1997, pp. 87–88). Since that time the shoreline position has been stable, in presumed sediment equilibrium (Komar, 1997). Changes in beach front morphology since that time can be explained by natural variability within the coastal system at this location (Komar *et al.*, 1976).

The ventifacts are located over a *c.* 30 m section of the south jetty and lie within the present-day intertidal zone of the adjacent beach (Figures 2b, 5). Two independent lines of evidence (outlined above) help constrain the possible age of the ventifacts: (1) historical changes in the position of mean high water (mapped by Komar *et al.*, 1976), and (2) construction and repair history of the jetty. Together, these show that the beach (which acted as the source region for wind-blown sand) and the jetty have both been essentially stable since about 1930. The ventifacts found at this location are therefore considered to have a maximum age of 60–70 years, but individual ventifacts may have formed prior to and since this time, and jetty repair and beach accretion may have changed boulder exposure. However, this is considered a best estimate supported by these two independent lines of evidence.

*Present wind regime and the calculation of abrasion rates*

The threshold velocity for sand transport by wind ($V_t$) can be calculated using the equation:

$$Vt = 680\sqrt{d}/\log(30/d)$$

where $d$ is the effective particle size (75 per cent of mean grain size) (Bagnold, 1941; Clark and Elson, 1961). Applying this equation to the beach sand samples shows that $V_t = 2{\cdot}82$ m s$^{-1}$. The consistent south-to-north orientation of the ventifacts clearly indicates that the location of abrasive sand transported by the wind is the adjacent beach to the south (Figures 2b, 3b). Winds above the threshold velocity ($V_t$, determined above), and from the southerly quadrant (between 135 and 225°), occur for 21·9–29·6 per cent of the time over the 108 months of wind data examined (8·5–10·2 per cent and 13·3–19·7 per cent of the time during the summer

 

and winter respectively over this time period) (Table II). However, there is considerable interannual variability in the frequency of southerly winds. Maximal values across the three weather stations range between 26·3 and 32·9 per cent annually, and minimal values between 13·9 and 26·1 per cent annually. The timing of these maximal/minimal values also fits with the El Niño/Southern Oscillation (ENSO) cycle which affects wind climate patterns throughout the east Pacific region. This wind variability therefore suggests there may be considerable variation in wind abrasion rate on an annual basis.

Overall rate of wind abrasion ($A_w$ in mm $a^{-1}$) can be calculated based on field estimates of the depth of rock removal from boulder surfaces ($R$ in mm), time period of ventifaction ($T$ in years) and the frequency of winds ($F$ expressed as a percentage of time) above the threshold velocity for winds transport (Table II) using the equation:

$$A_w = R/(TF/100)$$

$R$ was measured in the field as the relative relief (amplitude) of groove and ridge features. Relief was measured at a number of locations across the windward face of individual boulders, and the values were averaged. Relief varies markedly across individual boulders, with a maximum of $c.$ 25 mm depth recorded, but calculated mean values are generally consistent between boulders. $T$ is on the order of 70 years, and $F$ varies between 21·9 and 29·6 per cent across the wind datasets (Table II). We therefore calculate a range of values for $A_w$ based on variations in $R$ and $F$ (Table III). Mean values of $R$ yield abrasion rates in the range 0·72–0·96 mm $a^{-1}$ are consistent with some laboratory experiments (e.g. Schoewe, 1932), but theoretical and field ventifaction rates, from a range of geomorphic settings, vary over more than four orders of magnitude (e.g. Kuenen, 1928, 1960; Hickox, 1959; Suzuki and Takahashi, 1981; Miotke, 1982; Greely and Iversen, 1985). Sharp's (1964, 1980) experimental field results also yielded highly variable abrasion rates between different lithologies and on different time-scales, which was attributed to a dramatic increase in sand transport by wind towards the end of the study period (Sharp, 1980). These abrasion rates are shown in Table III for comparison with the examples described in this paper. The very much higher rates identified by Sharp can be related to higher sand transport by wind in semi-arid environments (Lancaster, 1984) and the relatively soft materials used. Such variability in abrasion rate therefore makes it more difficult to identify 'mean' abrasion rates especially where there is little control on ventifact age.

### *Significance of the results*

Previous work suggests that ventifacts generally form over long time-scales and may be geomorphically relict features (Sharp, 1949; Schlyter, 1995). The present paper provides the first well-constrained estimate of ventifaction rates from a modern coastal environment. As such, it sets the standard for comparison with other geomorphically active coasts. The calculated range of wind abrasion rates (Table III) is reasonable, but the least well-constrained parameter is abrasion depth ($R$) which is difficult to estimate from field examples. More precise field and laboratory experiments are therefore needed. It is also possible that ventifacts recorded from former periglacial environments (e.g. Christiansen and Svensson, 1998) could have formed very rapidly under similarly high abrasion rates.

The formation of ventifacts over short historical time-scales in Oregon also has implications for assessing coastal zone dynamics in similar coastal settings. This study shows that ventifacts may be sensitive proxy records of decadal-scale coastal zone changes on sandy tectonically active or formerly glaciated coasts. Future research strategies may include comparing rates of modern sand dune development and/or wind regimes to the record of blown sand as derived from coastal ventifacts.

## CONCLUSIONS

The presence of ventifacts on part of the south jetty of the Siuslaw River, central Oregon coast, attests to vigorous wind abrasion since jetty construction, mainly in the period 1930–present (70 years).

Based on ventifact orientation and estimated depth of rock removal, wind abrasion took place mainly by south-to-north winds during the winter, with a sand source on the adjacent beach. Using a standard equation

 

Table III. (A) Calculated rate of wind abrasion ($A_w$ in mm $a^{-1}$) based on averaged depth of surface rock loss ($R$). (B) Experimental wind abrasion rates obtained in the field, recalculated from Sharp (1964, 1980)

(A)

| Rock surface loss ($R$) (mm) | Frequency ($T$) of southerly winds above $V_t$(%) | | |
|---|---|---|---|
| | 21·9% (Newport) | 26·2% (Yaquina Bay) | 29·6% (Cape Arago) |
| 5 | 0·32 | 0·27 | 0·24 |
| 10 | 0·65 | 0·54 | 0·48 |
| 15 | 0·97 | 0·81 | 0·72 |
| 20 | 1·30 | 1·09 | 0·96 |
| 25 | 1·63 | 1·36 | 1·20 |

(B)

| Material | Abrasion rate (mm $a^{-1}$) | Time-period (years) | Reference |
|---|---|---|---|
| Lucite rod | 0·09 | 10 | Sharp(1964) |
| | 1·86 | 15 | Sharp(1980) |
| Red house | 6·77 | 6 | Sharp(1964) |
| Brick | 5·19 | 11 | Sharp(1964) |
| Gypsum | 4·82 | 10 | Sharp(1964) |
| Cement block | 3·4–36 | 15 | Sharp(1980) |
| Gneissic boulder | 0 | 10 | Sharp(1964) |

and grain size data from the beach the threshold for sand transport at this location is 2·82 m $s^{-1}$. Winds of this direction and exceeding this velocity are exceeded by 21·9–29·6 per cent of regional winds annually.

Based on ventifact and wind climate data, the wind abrasion rate at this locality is calculated to be in the order of 0·24–1·63 mm $a^{-1}$, dependent on abrasion depth. This is the first accurate and well-documented field estimate of wind abrasion in a modern coastal environment.

## ACKNOWLEDGEMENTS

Fieldwork in 1999 and 2000 for J.K. was funded partly by the School of Environmental Studies, University of Ulster.

## REFERENCES

Bagnold RA. 1941. *The Physics of Blown Sand and Desert Dunes*. Chapman and Hall: London.

Bishop DG, Mildenhall DC. 1994. The geological setting of ventifacts and wind-sculpted rocks at Mason Bay, Stewart Island, and their implications for late Quaternary paleoclimates. *New Zealand Journal of Geology and Geophysics* **37**: 169–180.

Blackwelder E. 1929. Sandblast action in relation to the glaciers of the Sierra Nevada. *Journal of Geology* **37**: 256–260.

Bond NA, Mass CF, Overland JE. 1996. Coastally trapped wind reversals along the United States west coast during the warm season. Part I: Climatology and temporal evolution. *Monthly Weather Review* **124**: 430–445.

Braley SM, Wilson P. 1997. Ventifacts from the coast of Northumberland. *Proceedings of the Geologists' Association* **108**: 141–147.

Christiansen HH, Svensson H. 1998. Windpolished boulders as indicators of a Late Weichselian wind regime in Denmark in relation to neighbouring areas. *Permafrost and Periglacial Processes* **9**: 1–21.

Clark TH, Elson JA. 1961. Ventifacts and eolian sand at Charette, P.Q. *Transactions of the Royal Society of Canada, Series III* **55**: 1–11.

Clemens KE, Komar PD. 1988. Oregon beach-sand compositions produced by the mixing of sediments under a transgressing sea. *Journal of Sedimentary Petrology* **58**: 519–529.

Cooper WS. 1958. *Coastal Sand Dunes of Oregon and Washington*. *Geological Society of America Memoir*, **72**.

Fisher TG. 1996. Sand-wedge and ventifact palaeoenvironmental indicators in north-west Saskatchewan, Canada, 11 ka to 9·9 ka BP. *Permafrost and Periglacial Processes* **7**: 391–408.

 

Fox WT, Davis RA. Jr. 1978. Seasonal variation in beach erosion and sedimentation on the Oregon coast. *Geological Society of America Bulletin* **89**: 1541–1549.
Greeley R, Iversen JD. 1985. *Wind as a Geological Process on Earth, Mars, Venus and Titan*. Cambridge University Press: Cambridge.
Hickox CF. 1959. Formation of ventifacts in a moist, temperate climate. *Bulletin of the Geological Society of America* **70**: 1489–1490.
Hunter RE, Richmond BM, Alpha TR. 1983. Storm-controlled oblique dunes of the Oregon coast. *Geological Society of America Bulletin* **94**: 1450–1465.
King LC. 1936. Wind-faceted stones from Marlborough, New Zealand. *Journal of Geology* **44**: 201–213.
Komar PD. 1997. *The Pacific Northwest Coast. Living with the Shores of Oregon and Washington*. Duke University Press: Durham, NH.
Komar PD, Lizarraga-Arciniega JR, Terich TA. 1976. Oregon coast shoreline changes due to jetties. *Journal of the Waterways, Harbors and Coastal Engineering Division* **102**: 13–30.
Kuenen PH. 1928. Experiments on the formation of wind-worn pebbles. *Leidsche Geologische Medellinger* **3**: 17–38.
Kuenen PH. 1960. Experimental abrasion 4: eolian action. *Journal of Geology* **68**: 427–449.
Laity JE. 1987. Topographic effects on ventifact development, Mojave Desert, California. *Physical Geography* **8**: 113–132.
Lancaster N. 1984. Characteristics and occurrence of wind erosion feature in the Namib Desert. *Earth Surface Processes and Landforms* **9**: 469–478.
Mass CF, Bond NA. 1996. Coastally trapped wind reversals along the United States west coast during the warm season. Part II: Synoptic evolution. *Monthly Weather Review* **124**: 446–461.
Maxson JH. 1940. Fluting and faceting of rock fragments. *Journal of Geology* **48**: 717–751.
Miotke F-D. 1982. Formation and rate of formation of ventifacts in Victoria Land, Antarctica. *Polar Geomorphology* **6**: 98–113.
Ritter DF, Dutcher RR. 1990. Geomorphic controls on the origin and location of the Tolman Ranch ventifact site, Park County, Wyoming, USA. *Journal of Geology* **98**: 943–954.
Schlyter P. 1995. Ventifacts as palaeo-wind indicators in southern Scandinavia. *Permafrost and Periglacial Processes* **6**: 207–219.
Schoewe WH. 1932. Experiments on the formation of wind-faceted pebbles. *American Journal of Science* **140**: 111–134.
Sharp RP. 1949. Pleistocene ventifacts east of the Big Horn Mountains, Wyoming. *Journal of Geology* **57**: 175–195.
Sharp RP. 1964. Wind-driven sand in Coachella Valley, California. *Geological Society of America Bulletin* **75**: 785–804.
Sharp RP. 1980. Wind-driven sand in Coachella Valley, California: Further data. *Geological Society of America Bulletin* **91**: 724–730.
Suzuki T, Takahashi T. 1981. An experimental study of wind abrasion. *Journal of Geology* **89**: 23–36.
USDA Soil Conservation Service. 1975. *Beaches and Dunes of the Oregon coast*. US Soil Service: Portland, OR.
Whitney MI, Dietrich RV. 1973. Ventifact sculpture by windblown dust. *Geological Society of America Bulletin* **84**: 2561–2582.

 